Water Supply

Water Supply Vol 22 No 4, 4544 doi: 10.2166/ws.2022.116

Analysis of rainfall and temperature characteristics and its correlation with Southern Oscillation Index in Beijing, China

Chengcheng Xu[a,b,*], Qingyan Sun[b] and Chuiyu Lu[b]

[a] School of Earth and Environment, Anhui University of Science and Technology, Huainan 232001, China
[b] State Key Laboratory of Simulation and Regulation of Water Cycle in River Basin, China Institute of Water Resources and Hydropower Research, Beijing 100038, China
*Corresponding author. E-mail: 1647203047@qq.com

ABSTRACT

In recent years, the urban area has continued to develop, and the demand for water resources is increasing. Rainfall, as an important source of water resources, is gaining more and more attention. Under this background, it is very necessary to analyse the changes in rainfall in Beijing, the capital of China. This study analysed the daily average temperature, rainfall data from 20 stations in the Beijing area in the past 50 years (1960–2012). Linear regression, mean variance, M-K method and ArcGIS spatial analysis are used to analyse Beijing's temperature and rainfall characteristics. These methods are applied to analyse the mutual relations between Beijing's rainfall, temperature changes and the Southern Oscillation Index (SOI). The results show that in the past 50 years in Beijing, the precipitation has shown a downward trend, the temperature has generally shown an upward trend, and the evaporation has generally shown a downward trend. The interrelation between regional climate change and the SOI is not significant. In the past 50 years, urban development has been closely related to the reduction of rainfall and increase in temperature. This study responds to the urgent need for research on the rainfall and temperature.

Key words: Beijing, linear regression analysis, Mann-Kendall, rainfall, SOI, temperature

HIGHLIGHTS

- Different methods are used to analyse temperature and rainfall characteristics.
- The variation of rainfall and temperature in Beijing over the past 50 years was analysed.
- Different regions are affected differently by SOI, and the difference between North and South China is obvious.

1. INTRODUCTION

With global warming, climate change has attracted more and more attention from scholars around the world. In the 21st century, global precipitation and extreme precipitation are increasing; especially in mid-high latitudes of the northern hemisphere, the rainfall intensity and frequency have increased significantly (Singh *et al.* 2021; X. Zhang *et al.* 2021). Many scholars have invested in research on extreme climates (Tye *et al.* 2016; Wu & Qian 2017; John *et al.* 2020). To deal with different geographical locations, different temperature zones, the selected methods are also different (Chen *et al.* 2020; Zander *et al.* 2020). In the application of methods, many researchers (Sugiyama *et al.* 2010; Mousavi *et al.* 2019) favour numerical simulation analysis and prediction. For the summer in the northern hemisphere, when rainfall increases significantly, targeted statistical methods are appropriate (Cunderlik & Burn 2002; Baratti *et al.* 2012; Li *et al.* 2021; Xu *et al.* 2021), but for the analysis of multiple seasons throughout the year, this method has many shortcomings. Many scholars use the frequency occurrence rate in mathematical statistics to solve this problem (Lee *et al.* 2012; Lu *et al.* 2019). In the 1970s, the Mann-Kendall method was applied to the field of hydrometeorological research (Kendall, l975), which included seasonal analysis and non-seasonal analysis (Hirsch *et al.* 1982). For the area of Beijing, China, several scholars have done some analysis on water resources (He *et al.* 2019). However, there are deficiencies in analysing climate change characteristics and trends. Research on the correlation between rainfall and SOI has been carried out in depth for the Yangtze River, but there are few studies on the area north of the Yangtze River (Tong 2006; Bradley *et al.* 2015; Li *et al.* 2021; Zhu *et al.* 2021). On the basis presented above, this article uses the non-seasonal Mann-Kendall method to mathematically process the collected rainfall data to analyse the characteristics of rainfall and temperature changes in Beijing over the past 50 years, as well as trend analysis. Combined with the Southern Oscillation Index (SOI), which affects rainfall as a factor, the SOI value is correlated with rainfall and temperature (Zhang *et al.* 2007; Dezfuli *et al.* 2010; Han *et al.* 2021). Due to insufficient consideration of the continuity of data in previous studies, this article uses the Kriging interpolation method to improve the station data in the Beijing area for nearly 50 years, and obtains continuous daily change data. Reliable basic data makes the results of this study more accurate and the conclusions more convincing.

2. INFORMATION AND METHODS

2.1. Regional overview and information

Beijing is located at 115.7°–117.4° E and 39.4°–41.6° W. The centre is located at 39°54′20″ W and 116°25′29″ E, with a total area of 16,410.54 km^2. The mountains surround the west, north and northeast, and the southeast is a great plain that slopes slowly towards the Bohai Sea. The summer of Beijing is hot and rainy, and the winter is cold and dry. Distribution of rainfall during the year is very uneven. The altitude of the Beijing Plain is 20–60 m, the mountain is generally 1,000–1,500 m above sea level, and the Dongling Mountain on the border with Hebei is 2,303 m above sea level, which is the highest peak in Beijing. There are four main rivers in Beijing, respectively Chaobai River, Beiyun River, Yongding River and Juma River. The Beijing area is shown in Figure 1. In this study, the daily average temperature, precipitation, humidity, sunshine and wind speed data from 20 survey sites in the Beijing area in the past 50 years (1960–2012) are used for analysis.

2.2. Data quality control

(1) Extreme value control

Each element of the automatic weather station has a certain climatic extreme value range. By combining the climatic extreme value range of the element and the regional topographic characteristics, the monthly extreme value threshold $V_{\max}$ and $V_{\min}$ of each element are set; when the observed value $V > V_{\max}$ or $V < V_{\min}$, the observed value is wrong and will be deleted. By extreme value controlling, the threshold of each element is dynamically changed according to the change of the month.

(2) Time continuity control

Climate elements have their own evolutionary laws, and the elements fluctuate within a certain range in adjacent periods. The time continuity control method uses hours as the time interval, combined with the change law of each element itself and the experience value over the years, and sets the hourly change threshold (V_h) of each element. When the observation value $V \geq 2\ V_h$, the observation value is considered to be wrong; when $V \leq 0.5\ V_h$, the observation value is also considered to be wrong, and these data will be deleted.

(3) Kriging interpolation method

Kriging interpolation method (Kriging), known as spatial local interpolation method, is based on the theory of variogram and structural analysis. A method of unbiased optimal estimation of regionalized variables in a limited area is one of the main contents of geostatistics. The scope of application of the Kriging interpolation method is the spatial correlation of regionalized variables. If the results of the variogram and structural analysis show that the regionalized variables are spatially related, the Kriging method can be used for interpolation or extrapolation; otherwise, it is not feasible. The essence is to use the original data of regionalized variables and the structural characteristics of the variogram to make linear unbiased and optimal estimation of unknown samples.

(4) Thiessen polygon

Thiessen polygon is a subdivision of the space plane. Its characteristic is that any position in the polygon is the closest to the sample point of the polygon (such as the hydrological station), and the distance to the sample point in the adjacent polygon is far. The polygon contains only one sample point. Because of the equipartition characteristics of the Thiessen polygon in the spatial division, it can be used to solve problems such as the nearest point, the smallest closed circle, and many spatial analysis problems, such as adjacency, proximity, and reachability analysis.

2.3. Calculation method

2.3.1. Mann-Kendall

Rainfall and runoff analysis use the Mann-Kendall (M-K) test method to detect the long-term precipitation trends and sudden changes in the stream basin. In the series of time trend, Mann and Kendall originally proposed the test method. Many scholars continue to use the M-K method to analyse the series of time trend changes of factors such as precipitation, runoff, temperature, and water quality. M-K test does not require the sample to follow a certain distribution, nor is it disturbed by a few outliers. It is suitable for non-normally distributed data such as hydrology and meteorology which is easy to calculate.

In the M-K test, $(X_1..., X_n)$ represents a time series, and the n in the time series is independent, random variables and has a changeless distribution. In the matrix, for all $k, j \leq n$, and k not equal to j, the X_k and X_j is different in distribution, the statistical S of the test can be obtained from the formula:

$$S = \sum_{k=1}^{n-1} \sum_{j=k+1}^{n} \mathrm{Sgn}(X_j - X_k) \tag{1}$$

where,

$$Sgn(X_j - X_k) = \begin{Bmatrix} +1 & (X_j - X_k) > 0 \\ 0 & (X_j - X_k) = 0 \\ -1 & (X_j - X_k) < 0 \end{Bmatrix} \tag{2}$$

S is a normal distribution with a mean of 0. When $n > 10$, the standard normal system variable can be obtained from the formula:

$$Z = \begin{Bmatrix} \dfrac{S-1}{\sqrt{V_{\alpha r}(S)}} & S > 0 \\ 0 & S = 0 \\ \dfrac{S+1}{\sqrt{V_{\alpha r}(S)}} & S < 0 \end{Bmatrix} \tag{3}$$

For further use of the M-K test such as detecting sequence mutations, the result can be obtained from the formula:

$$S_k = \sum_{i=1}^{k} \sum_{j}^{i-1} \alpha_{ij} \quad (k = 2, 3, 4, \ldots, n) \tag{4}$$

where,

$$\alpha_{ij} = \begin{cases} 1 & X_i > X_j \\ 0 & X_i < X_j \end{cases} \quad 1 \leq j \leq I \tag{5}$$

Define statistical variables:

$$UF_k = \frac{[S_k - E(S_k)]}{\sqrt{V\alpha r(S_k)}} \quad (k = 1, 2, \ldots, n) \tag{6}$$

where,

$$E(S_\mathrm{k}) = \mathrm{k}(K+1)/4; \, V_{\alpha r}(S_k) = k(k-1)(2k+5)/72 \tag{7}$$

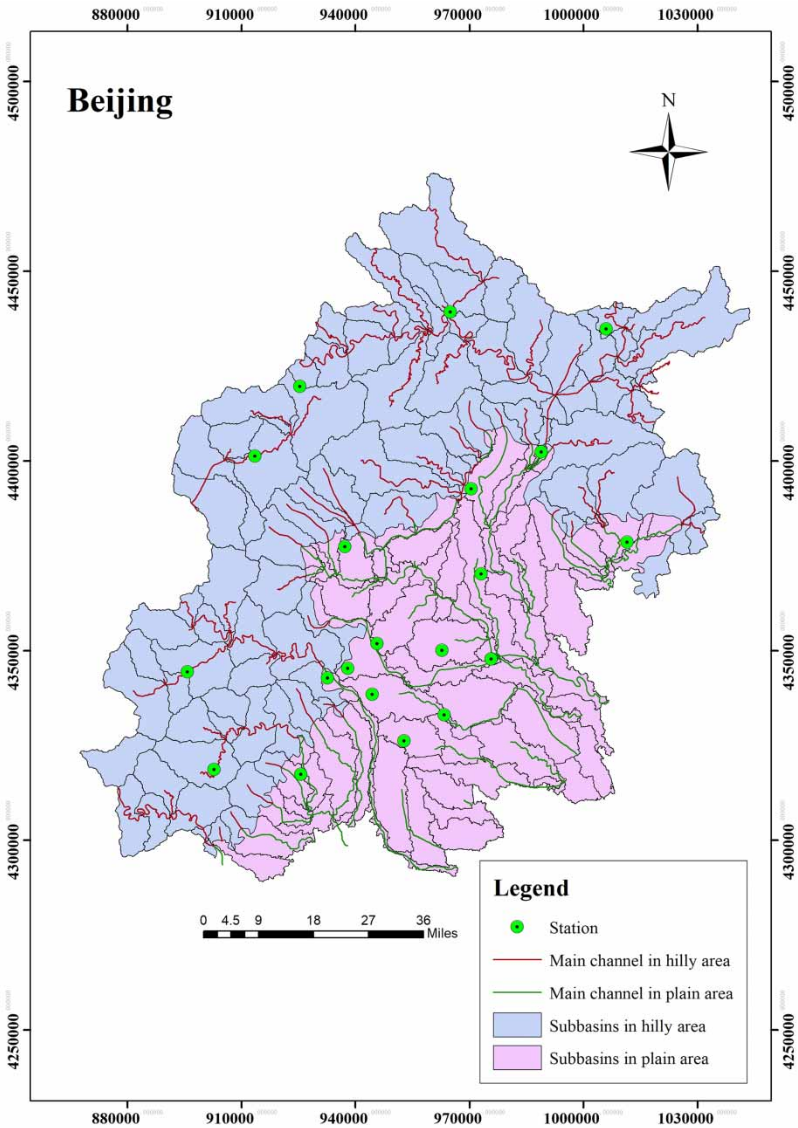

Figure 1 | Beijing hydrological station information.

The time series x is arranged in reverse order, and then calculated according to the above formula, while making:

$$\begin{cases} UB_{\mathrm{k}} = -UF_{\mathrm{k}} \\ \mathrm{k} = \mathrm{n} + 1 - k \end{cases} \quad (\mathrm{k} = 1, 2, \ldots, \mathrm{n}) \tag{8}$$

2.3.2. Cumulative anomaly method

For the time series x, the formula for its accumulated anomaly at a certain time is as follows:

$$y_t = \sum ti = 1(xi - x), t = (1, 2, \ldots, n) \tag{9}$$

where: xi is the value of the time series of the temperature element at i; x is the average value of the time series. According to the accumulated anomaly value at different moments, the accumulated anomaly curve can be drawn.

2.3.3. Linear regression analysis

(1) Model establishment and parameter estimation

According to relevant background knowledge or scatter plots, if the two variables are approximately linearly related, a univariate linear regression model can be used:

$$y = \beta_0 + \beta_1 x + \varepsilon \tag{10}$$

where y is called the explanatory variable (dependent variable), x is the explanatory variable (independent variable), $\beta_0, \ \beta_1$ are regression coefficient, and ε is the random error.

Using the least square method, the estimated value of $\beta_0, \ \beta_1$ can be obtained.

(2) Significance test of regression analysis

- (i) Using the F statistic to test the significance of the regression equation is a common method.
  For a given significance level, a, corresponding to Fa, if the F value calculated from the sample satisfies $F > Fa$, the hypothesis (not significant) is rejected, that is, the regression equation is significant at a level.
- (ii) Using the T statistic to test the significance of the regression equation is another common method.

When the overall data presents a normal distribution, if the total data standard deviation is unknown and the sample size $n < 30$, then the dispersion statistics of all possible sample averages and population averages at this time are t-distributed.

The t test uses the t-distribution theory to infer the probability of the difference, to compare whether the difference between the two averages is significant. When the sample $n < 30$, the test formula is:

$$t = (\bar{x} - \mu)/\left(\delta_x/\sqrt{n-1}\right) \tag{11}$$

when the sample $n > 30$, the test formula is:

$$t = (\bar{x} - \mu)/(\delta_x/\sqrt{n}) \tag{12}$$

Here,

t is the deviation statistic;
$\bar{x}$: sample average;
μ: overall average;
δ_x: sample standard deviation;
n: sample size.

3. RESULTS

Using the linear trend analysis method to combine the data analysis of 20 meteorological stations in Beijing over 50 years, and using the ArcGIS spatial analysis function to perform Thiessen polygon processing (Figure 2), the weight of each station control (Table 1) was obtained, and mathematical statistical analysis was performed.

From the rainfall and temperature data in Table 2, we can see that some stations have missing data, but the total amount missing is less than 5%.

Due to the long data period, and the site layout is not uniform, some of the site data are missing. The Thiessen polygons method can be used to solve this problem. Combined with the weight of each site, the rainfall, temperature, humidity, and sunshine data in Beijing are obtained (Table 3).

It can be seen from the Cv value that the coefficient of variation of the temperature and rainfall data in Beijing is much greater than 4%, indicating that the data are irregular between years and relatively discrete. For rainfall, Cs value is positive, indicating that the number less than the mean appears more frequently; for temperature, the Cs value is positive, indicating that the number less than the mean appears less frequently. The large differences of some years indicate that the climate in Beijing has experienced a certain climate change in recent years. The annual average rainfall maximum value mostly appeared in 1995, and the annual average temperature maximum value appeared in 1999.

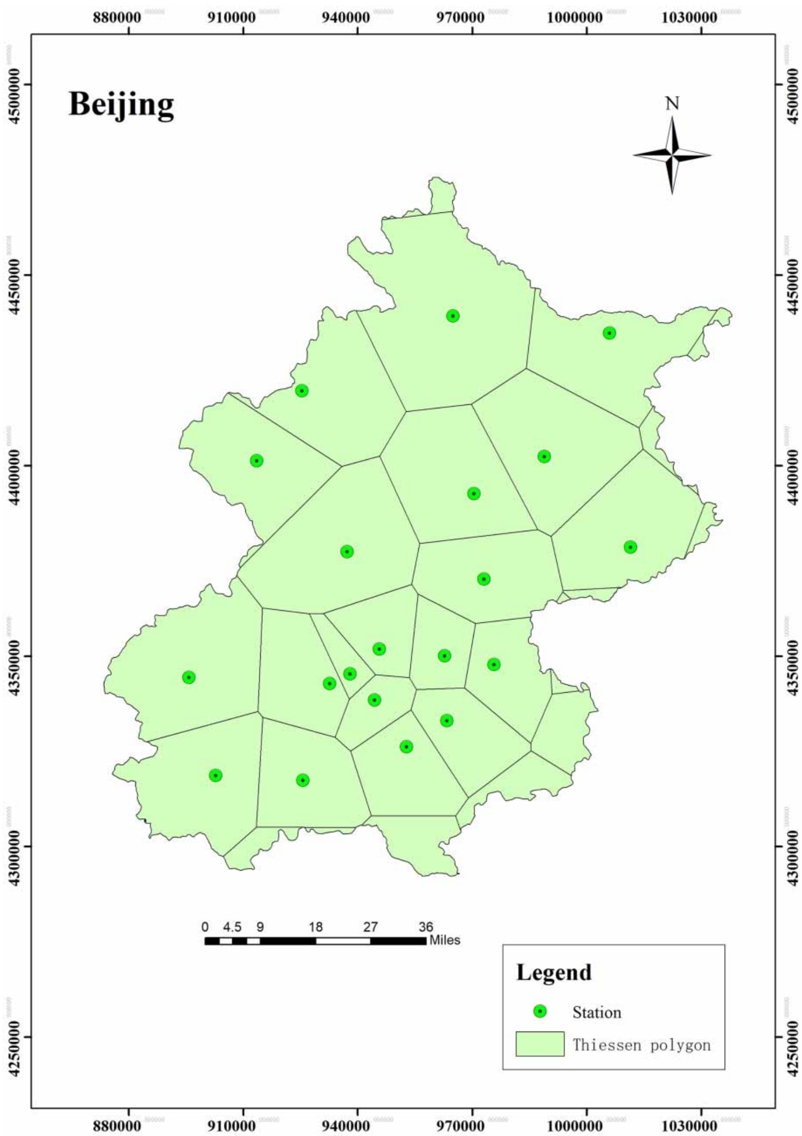

Figure 2 | Thiessen division.

3.1. Variation analysis

3.1.1. Trend analysis and test

Using the M-K test method to analyse the rainfall and temperature trends and continuity in Beijing, the result of rainfall is shown in Figure 3, and the result of temperature is shown in Figure 4. The analysis of meteorological parameters sequence in Beijing is shown in Table 4.

For the rainfall analysis, the value of confidence level is $1.26 < |Z| < 1.64$ and it is a negative value. The calculation results are shown in Figure 5(a). According to the M-K test, the credibility is 90%, which reveals that the rainfall data of 50 years has a significant reduction trend; for the temperature analysis, the value of confidence level is $1.64 < |Z| < 2.32$ and it is a positive value; according to the M-K test, the credibility is 95%, which indicates a significant increase in temperature. The calculation results are shown in Figure 5(b).

Through the M-K test, the intersection point of the two curves UF(k) and UB(k) between the confidence levels is the abnormal year within the corresponding year, and the rainfall abnormal years are: 1981, 1985–1987, 1989, 2007, 2010; the years of abnormal temperature are: 1982, 1985, 1993, 1995, 2003, 2010.

Table 1 | Thiessen polygons weight analysis

Station	Mentougou	Tongxian	Miyun	Yanqin	Tanghekou	Xiayunling	Fangshan	Daxing	Fengtai	Shijingshan
Weights	0.038444	0.050044	0.072112	0.055661	0.088542	0.051945	0.044631	0.04221	0.016115	0.009441
Station	**Zhaitang**	**Haidian**	**Beijing**	**Zhaoyang**	**Shunyi**	**Pinggu**	**Shangdianzi**	**Huairou**	**Changping**	**Foyeding**
Weights	0.066582	0.024433	0.045737	0.021331	0.049786	0.058483	0.056145	0.065408	0.082109	0.060841

Table 2 | Completeness of the precipitation data

Number of missing data in one day	Total number of missing days in 1960–2012	The proportion of missing sites	Missing time
[0,10)	994	0.00	—
[10,20)	818	0.05	—
[20,30)	567	0.10	—
[30,40)	370	0.15	—
[40,50)	168	0.20	—
[50,60)	89	0.25	—
[60,70)	66	0.30	—
[70,80)	26	0.36	1978/6/13,1978/7/14,1979/6/4,1979/7/7,1980/7/31,1983/6/24,1984/6/20,1986/6/13,1988/6/27,1988/7/8,1988/7/30,1997/6/2,1993–1994/6/5,1994/6/28,1995/8/31,2001/6/11–12,2002/8/30,2006/6/19,
[80,90)	15	0.41	1979/6/1,1997/6/10,1980/7/3,1982/7/10,1983–1984/6/4,1984/7/19,1984/7/31,1987/6/25,1988/8/31,2004/6/4,2008/8/31
[90,100)	11	0.46	1978/6/5,1983/6/11,1990/6/17,1990/8/18,1992/6/11,1995/7/31,2002/7/30,2003/7/31,2009/8/31
[100,197)	4	0.51	1982/8/31,1983/6/16,1993/6/21,2002/6/30

3.1.2. Data validation

In the calculation of time series variation analysis, because the M-K test does not require samples to follow a certain distribution and is not disturbed by a few outliers, the M-K test is often preferred in the analysis of climatic parameters and hydrological sequence variation by researchers. However, the M-K curve often has multiple points crossing and overlapping. As shown in Figure 5(a) and 5(b), the two curves of rainfall and temperature UF(k) and UB(k) have multiple points crossing in the statistical year, which is difficult to accurately to find the point of variation. In order to verify the accuracy of the variation, this paper uses the cumulative anomaly method to verify the evaporation variation point based on the Mann-Kendall test. Figure 6(a) and 6(b) shows the analysis curve of cumulative anomaly rainfall and temperature in Beijing.

It can be seen from Figure 6(a) and 6(b), calculated by the cumulative anomaly method, the year of rainfall variation is 1979, 1981, 1983, 1985, 1988–1991, 1994–2000, 2002–2003, 2005, 2009, 2010. The year of temperature variation is 1977, 1983, 1985–1986, 1989–1993, 1995, 1998–1999, 2002, 2004–2010. Combining the M-K test and the cumulative anomaly method, referring to the statistics of the overall trend of each parameter index during the year, the final determination of the variation of each parameter in Beijing is shown in Table 5.

Table 3 | Characteristic value of meteorological data

	min	max	Cv	Cs
Year	1976	1995	0.1876	0.1027
Rainfall (mm)	351.7	753.675		
Year	1988	1999	0.1746	– 0.0421
Temperature (°C)	−29.5	41.7		
Year	2005	1991	0.0597	1.3329
Relative humidity	51.4055	69.6219		
Year	2006	1983	0.0667	0.1872
Sunshine time (h)	6.0517	7.8885		
Year	2014	2014	0.1118	– 0.2551
Wind speed (m/s)	1.7116	1.7116		

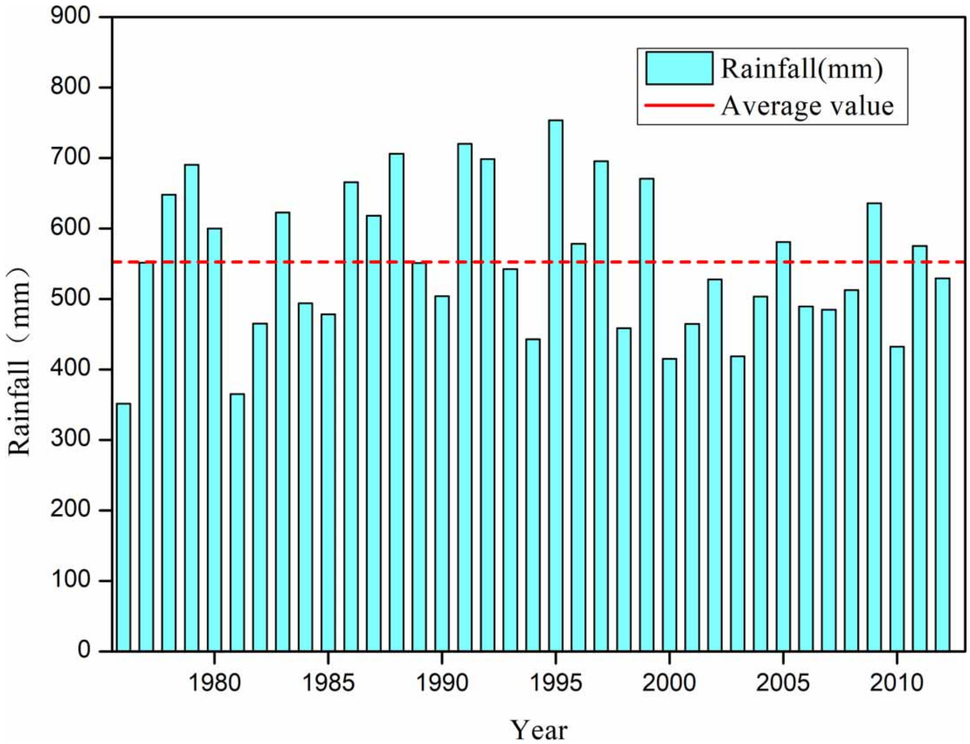

Figure 3 | Rainfall trends of each year.

3.2. Correlation analysis of Southern Oscillation Index (SOI)

It is found that there is a negative correlation between SOI and rainfall and temperature. When *a* equals 0.05, the relationship between rainfall-temperature and SOI in Beijing is not significant. In this paper, F-test and T-test are used to make relevant

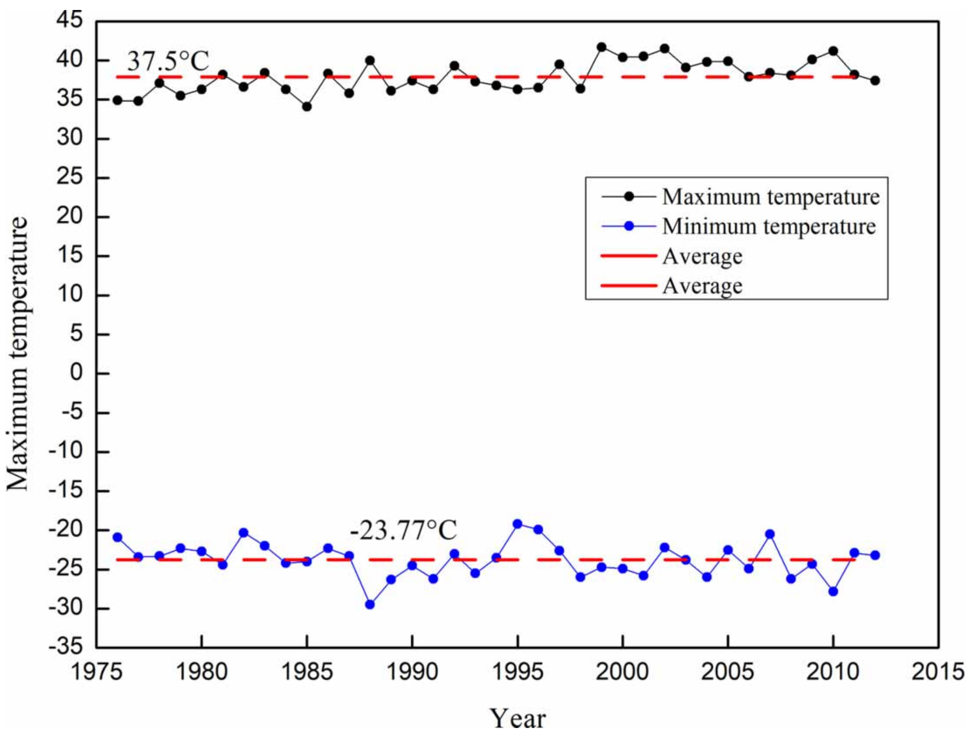

Figure 4 | Temperature change of each year.

Table 4 | Analysis of meteorological parameters sequence in Beijing

Analysis object	Confidence level (Z)	Confidence	Trend
Rainfall	−1.43867693	90%	Significantly reduced
Temperature	1.804885604	95%	Significantly increased

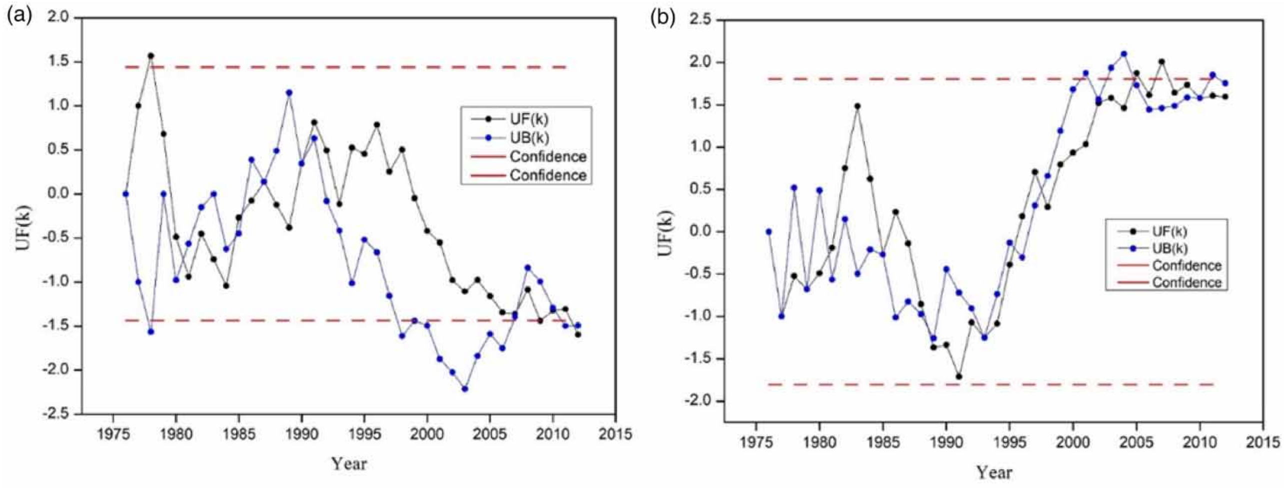

Figure 5 | (a) Mann-Kendall curve of rainfall variation. (b) Mann-Kendall curve of temperature variation.

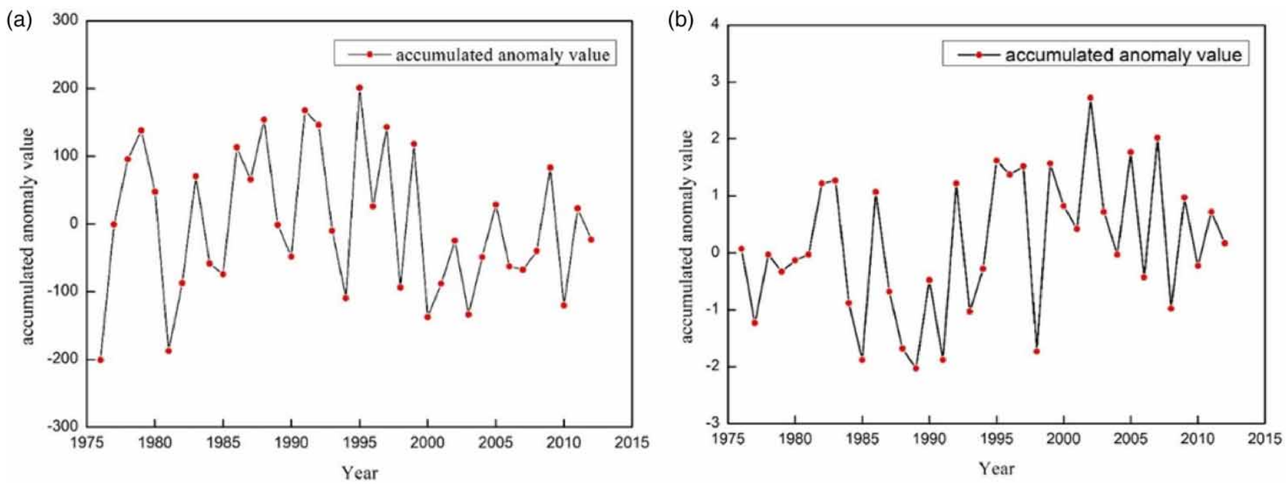

Figure 6 | Variation curve. (a) Rainfall variation curve. (b) Temperature variation curve.

Table 5 | Variation year statistics in Beijing

	Mann-Kendall	Cumulative anomaly	Comprehensive
Rainfall	1981, 1985–1987, 1989, 2007, 2010	1984, 1992, 1979, 1981, 1983, 1985, 1988–1991, 1994–2000, 2002–2003, 2005, 2009, 2010	1984, 1989, 2010
Temperature	1982, 1985, 1993, 1995, 2003, 2010	1977, 1983, 1985–1986, 1989–1993, 1995, 1998–1999, 2002, 2004–2010	1989, 1985, 1993, 1995, 2010

tests, and the results were found to be not significantly related, as shown in Tables 6–9. The histogram of rainfall distribution frequency is shown in Figure 7; the histogram of temperature distribution frequency is shown in Figure 8. Considering the geographical location of Beijing, this analysis shows that the Beijing area is less affected by the Southern Ocean climate.

From Table 6, $F = 1.887 < Fa\ (1, 35) = 4.12$, therefore, it is not significant at the 0.05 confidence level.
From Table 7, $F = 0.095 < Fa\ (1, 35) = 4.12$, therefore, it is not significant at the 0.05 confidence level.
From Table 8, $t = -1.374 < t\ (35) = 1.69$, therefore, it is not significant at the 0.05 confidence level.
From Table 9, $t = -0.309 < t\ (35) = 1.69$, therefore, it is not significant at the 0.05 confidence level.

Table 6 | F-test data of rainfall[b]

	Sum of squares	df	Mean square	F	Sig.
Regression	1203716.935	1	1203716.935	1.887	0.178[a]
Residual	2.23×10^7	35	637979.906		
Total	2.35×10^7	36			

[a]SOI.
[b]Rainfall.

Table 7 | F-test data of temperature[b]

	Sum of squares	df	Mean square	F	Sig.
Regression	0.147	1	0.147	0.095	0.759[a]
Residual	54.031	35	1.544		
Total	54.178	36			

[a]SOI.
[b]Temperature.

Table 8 | T-test data of rainfall[a]

					95% confidence interval	
	B	Standard error	t	sig.	Lower limit	Upper limit
Constant	4,383.665	137.839	31.803	0	4,103.836	4,663.493
SOI	−25.063	18.246	−1.374	0.178	−62.104	11.979

[a]Rainfall.

Table 9 | T-test data of temperature[a]

					95% confidence interval	
	B	Standard error	t	sig.	Lower limit	Upper limit
Constant	7.053	0.214	32.893	0	6.618	7.488
SOI	−0.009	0.028	−0.309	0.759	−0.066	0.049

[a]Temperature.

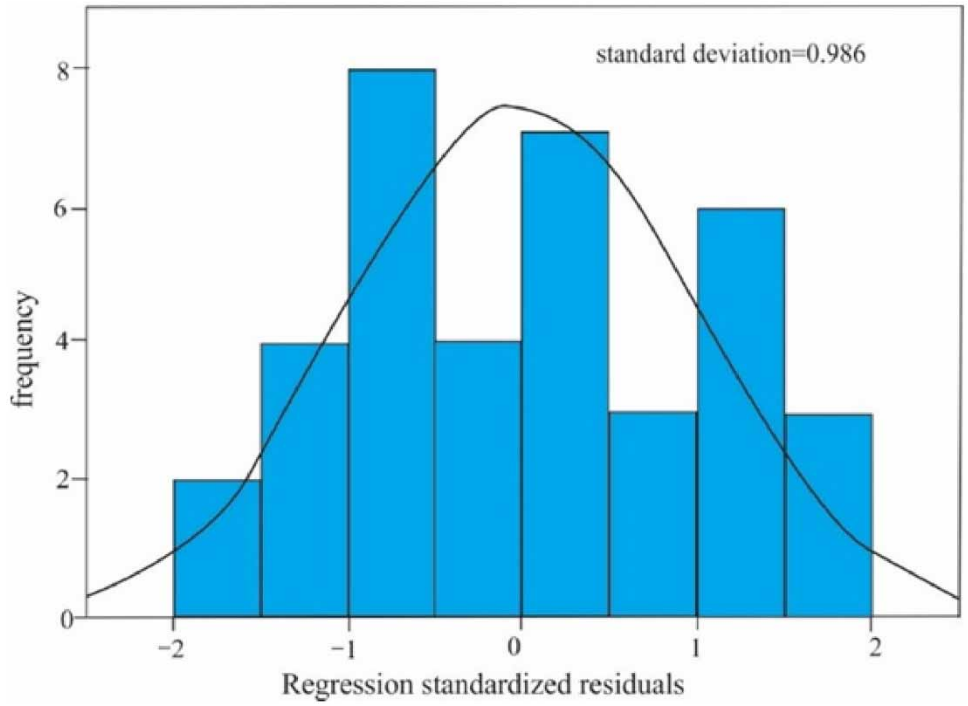

Figure 7 | Histogram of rainfall distribution frequency.

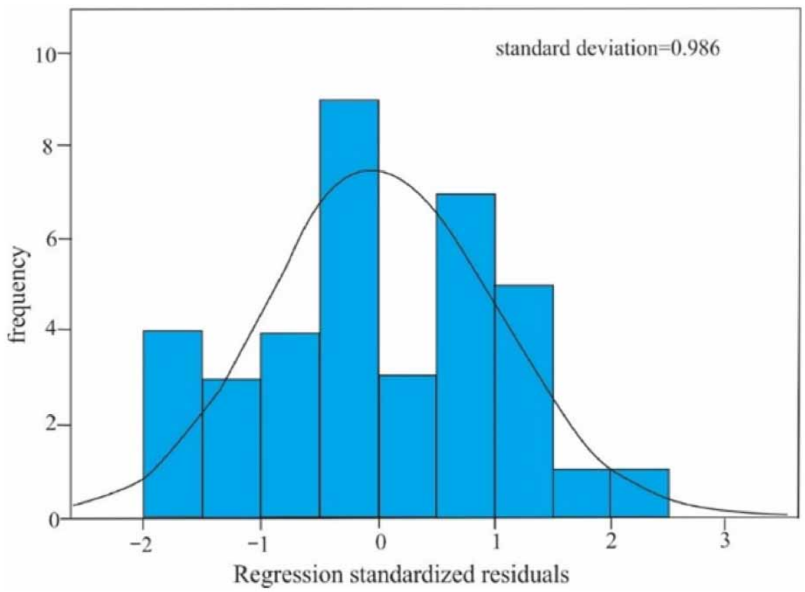

Figure 8 | Histogram of temperature distribution frequency.

4. DISCUSSION AND CONCLUSION

4.1. Discussion

Analysis of rainfall and temperature characteristics and its correlation with Southern Oscillation Index in a city like Beijing is necessary. The results of the analysis provide guidance for the region to respond to extreme climate change and prepare for prevention and control.

The variation characteristics of rainfall and temperature in Beijing are obtained by using M-K method. This method has been widely used in hydrological research. For Beijing area, some scholars have also analysed the trend of temperature and rainfall, and these results are relatively consistent (Liu *et al.* 2007; Shen & Xu 2021; Y. Zhang *et al.* 2021). However, in this study, the cumulative anomaly method is added to test the selection of mutation time points, which makes the results more accurate. For the study on the correlation between regional climate and Southern Oscillation Index, many scholars have selected different regions for research (Nazemosadat & Cordery 2015; Ghorbani *et al.* 2021). Due to the differences in selected regions, the final research conclusions are also quite different. Due to the highest evaporation recycling rate in the continent's windward regions (Keys *et al.* 2016), in the eastern part of the northern hemisphere, the eastern side of the North American and Eurasian continents experienced lower land evaporation cycles, resulting in less rainfall on land. For the global climate system, changes in land use in one region will also promote changes in another region. Considering the above factors and the study of rainfall in a region, reasonable management of regional water resources needs to be combined with the wind direction above the local region (Keys *et al.* 2017). There is great uncertainty in the changes of temperature and rainfall. In this study, Mann-Kendall and other methods are used to analyse the characteristics of rainfall and temperature changes in Beijing. The theoretical basis is reliable, but there are still some improvements in the calculation of this kind of method. For example, in the analysis of temperature change, there are some deviations in the final results, but these deviations are inevitable and acceptable.

4.2. Conclusion

During the 50 years in Beijing, rainfall has shown a clear decreasing trend, including anomalies in 1984, 1989, and 2010; temperature has shown a significant increasing trend, including anomalies in 1985, 1989, 1993, 1995, and 2010. The declining trend of rainfall shows that the area of Beijing in the future will experience reduced water resources year by year, and Beijing's domestic, industrial, and agricultural water resources must be well allocated.

Through mathematical analysis, it is found that the relationship between rainfall, temperature change and SOI in Beijing is not significant. Due to the geographical differences between the north and south in China, the climate of the southern area is greatly affected, and the north receives less influence.

COMPETING INTERESTS

There are no conflicts of interest to declare.

ACKNOWLEDGEMENTS

Thanks to the peers for the reviews of this paper. Financial support for the study was provided by Applied Technology Research and Development Program of Heilongjiang Province (grant No.GA19C005).

DATA AVAILABILITY STATEMENT

All relevant data are included in the paper or its Supplementary Information.

REFERENCES

Baratti, E., Montanari, A., Castellarin, A., Salinas, J. L., Viglione, A. & Bezzi, A. 2012 Estimating the flood frequency distribution at seasonal and annual time scales. *Hydrology and Earth System Sciences* **16** (12), 4651–4660.

Bradley, A., Habib, M. & Schwartz, S. 2015 Climate index weighting of ensemble streamflow forecasts using a simple Bayesian approach. *Water Resources Research* **51** (9), 7382–7400.

Chen, L., Chen, Z., Jia, G., Zhou, J., Zhao, J. & Zhang, Z. 2020 Influences of forest cover on soil freeze-thaw dynamics and greenhouse gas emissions through the regulation of snow regimes: a comparison study of the farmland and forest plantation. *Science of the Total Environment* **726**, 138403.

Cunderlik, J. M. & Burn, D. H. 2002 Analysis of the linkage between rain and flood regime and its application to regional flood frequency estimation. *Journal of Hydrology* **261** (1–4), 115–131.

Dezfuli, A. K., Karamouz, M. & Araghinejad, S. 2010 On the Relationship of Regional Meteorological drought with SOI and NAO over Southwest Iran. *Theoretical & Applied Climatology* **100** (1–2), 57–66.

Ghorbani, M. A., Kahya, E., Roshni, T., Kashani, M. H. & Heddam, S. 2021 Entropy analysis and pattern recognition in rainfall data, north Algeria. *Theoretical and Applied Climatology* **144**, 7263.

Han, Y., Ma, Y., Wang, Z., Xie, Z. & Fan, Y. 2021 Variation characteristics of temperature and precipitation on the northern slopes of the Himalaya region from 1979 to 2018. *Atmospheric Research* **253** (6), 105481.

He, G., Zhao, Y., Wang, J., Zhu, Y., Jiang, S., Li, H. & Wang, Q. 2019 The effects of urban water cycle on energy consumption in Beijing, China. *Journal of Geographical Sciences* **29** (6), 959–970.

Hirsch, R. M., Slack, J. R. & Smith, R. A. 1982 Techniques of trend analysis for monthly water quality data. *Water Resources Research* **18** (1), 107–121.

John, E., Walsh Thomas, J., Ballinger, A., Eugénie, S. & Euskirchen, B. 2020 Extreme weather and climate events in northern areas: a review. *Earth Science Reviews* **209**, 1–19. 103324.

Kendall, M. G. 1975 *Rank Correlation Methods*. Griffin, London.

Keys, P. W., Lan, W. E. & Gordon, L. J. 2016 Revealing invisible water: moisture recycling as an ecosystem service. *PLoS ONE* **11** (3), e0151993.

Keys, P. W., Lan, W. E. & Gordon, L. J. 2017 Approaching moisture recycling governance. *Global Environmental Change* **45**, 15–23.

Li, X., Sha, J. & Wang, Z. L. 2021 Influence of the Three Gorges Reservoir on climate drought in the Yangtze River Basin. *Environmental Science and Pollution Research International* **28** (23), 29755–29772.

Lee, J.-J., Kwon, H.-H. & Kimm, T. W. 2012 Spatio-temporal analysis of extreme precipitation regimes across South Korea and its application to regionalization. *Journal of Hydro-Environment Research* **6** (2), 101–110.

Liu, H. Z., Wang, W. G. & Shao, M. X. 2007 A case study of the influence of the western pacific subtropical high on the torrential rainfall in Beijing Area. *Chinese Journal of Atmospheric Sciences* **31** (4), 727–734.

Lu, S., Bai, X., Li, W. & Wang, N. 2019 Impacts of climate change on water resources and grain production. *Technological Forecasting and Social Change* **143** (6), 76–84.

Mousavi, M. S., Mirfendereski, S., Park, J. S. & Eun, J. 2019 Experimental and numerical analysis of a sustainable farming compartment with evaporative cooling system. *Processes* **7** (11), 823.

Nazemosadat, M. J. & Cordery, I. 2015 On the relationships between ENSO and autumn rainfall in Iran. *International Journal of Climatology* **20** (1), 47–61.

Shen, H. & Xu, Z. 2021 Monitoring and evaluating rainfall–runoff control effects of a low impact development system in future science park of Beijing. *JAWRA Journal of the American Water Resources Association* **57** (4), 638–651.

Singh, H., Najafi, M. R. & Cannon, A. J. 2021 Characterizing non-stationary compound extreme events in a changing climate based on large-ensemble climate simulations. *Climate Dynamics* **24**, 1–17.

Sugiyama, M., Shiogama, H. & Emori, S. 2010 Precipitation extreme changes exceeding moisture content increases in MIROC and IPCC climate models. *Proceedings of the National Academy of Sciences* **107** (2), 571–575.

Tong, J., Qian, Z. & Deming, Z. 2006 Yangtze floods and droughts (China) and teleconnections with ENSO activities (1470–2003). *Quaternary International* **144** (1), 29–37.

Tye, M. R., Blenkinsop, S., Fowler, H. J., Stephenson, D. B. & Kilsby, C. G. 2016 Simulating multimodal seasonality in extreme daily precipitation occurrence. *Journal of Hydrology* **537**, 117–129.

Wu, H. & Qian, H. 2017 Innovative trend analysis of annual and seasonal rainfall and extreme values in Shaanxi, China, since the 1950s. *International Journal of Climatology* **37**, 2582–2592.

Xu, C., Lu, C. & Sun, Q. 2021 Impact of climate change on irrigation water requirement of wheat growth – A case study of the Beijing-Tianjin-Hebei region in China. *Urban Climate* **39**, 100971.

Zander, S., Brousse, O. & Esau, I. 2020 Hyperlocal mapping of urban air temperature using remote sensing and crowdsourced weather data. *Remote Sensing of Environment* **242**, 111791.

Zhang, Q., Xu C, Y., Jiang, T. & Wu, Y. 2007 Possible influence of ENSO on annual maximum streamflow of the Yangtze River, China. *Journal of Hydrology* **333** (2–4), 265–274.

Zhang, X., Zheng, Z. & Wang, K. 2021 Prediction of runoff in the upper Yangtze River based on CEEMDAN-NAR model. *Water Supply* **21** (7), 3307–3318.

Zhang, Y., Gao, Y., Guo, L. & Zhang, M. 2021 Numerical analysis of aerosol direct and indirect effects on an extreme rainfall event over Beijing in July 2016. *Atmospheric Research* **264**, 105871.

Zhu, S., Li, D., Huang, G., Chhipi-Shrestha, G., Nahiduzzaman, K. M., Hewage, K. & Sadiq, R. 2021 Enhancing urban flood resilience: A holistic framework incorporating historic worst flood to Yangtze River Delta, China. *International Journal of Disaster Risk Reduction* **61**, 102355.

First received 8 September 2021; accepted in revised form 18 February 2022. Available online 2 March 2022